minerals

MDPI

Article

Mineral Quantification with Simultaneous Refinement of Ca-Mg Carbonates Non-Stoichiometry by X-ray Diffraction, Rietveld Method

Hélisson Nascimento dos Santos [1,*], Reiner Neumann [1,2] and Ciro Alexandre Ávila [2]

[1] CETEM—Centre for Mineral Technology, Division for Technological Characterisation, 22461-908 Rio de Janeiro, Brazil; rneumann@cetem.gov.br

[2] Museu Nacional, Universidade Federal do Rio de Janeiro, 20940-040 Rio de Janeiro, Brazil; avila@mn.ufrj.br

* Correspondence: helissonnsantos@gmail.com; Tel.: +51-21-3865-7263

Received: 3 July 2017; Accepted: 4 September 2017; Published: 8 September 2017

Abstract: Quantitative phase analyses of carbonate rocks containing Mg-rich calcite and non-stoichiometric dolomite by the Rietveld method yielded improved results when the substitutions are refined for either minerals. The refinement is constrained by the *c*-axis of the lattice for both minerals using the formula $c = -1.8603\ n\mathrm{Mg} + 17.061$ for calcite, where nMg is the molar fraction of Mg replacing Ca, and $c = 16.0032 + 0.8632\Delta n_{\mathrm{Ca}}$ for dolomite, with Δn_{Ca} being the excess Ca in its B site. The one-step procedure was implemented into the Topas software and tested on twenty-two carbonate rock samples from diverse geological settings, considered analogues to petroleum system lithotypes of the pre-evaporite deposits of Southeastern Brazil. The case study spans over a wide range of calcite and dolomite compositions: up to 0.287 apfu Mg in magnesian calcite, and Ca in excess of up to 0.25 apfu in non-stoichiometric dolomite, which are maximum substitutions the formulas support. The method overcomes the limitations for the quantification of minerals by stoichiometry based on whole-rock chemical analysis for complex mineralogy and can be employed for multiple generations of either carbonate. It returns the mineral quantification with unprecedented detailing of the carbonates' composition, which compares very well to spot analysis (both SEM-EDS and EMPA) if those cover the full range of compositions. The conciliation of the quantification results based on the XRD is also excellent against chemical analysis, thermogravimetry, and carbon elemental analysis.

Keywords: carbonates; magnesian calcite; non-stoichiometric dolomite; Rietveld method; X-ray diffraction

1. Introduction

Calcite and dolomite, the most common carbonate minerals, are ubiquitous in a great variety of sedimentary, metamorphic, and igneous rocks. Along the calcite-magnesite compositional series, dolomite, as the intermediary mineral equivalent to the reaction $CaCO_3 + MgCO_3 = CaMg(CO_3)_2$ boasts a cell volume decrease [1] of up to 12%, as compared to calcite [2]. Besides end-members and the intermediary phase, the continuous exchange of cations produces magnesian calcite ($Ca_{1-x}Mg_xCO_3$) and non-stoichiometric dolomite as the most important minerals.

The Mg content in magnesian calcite and dolomite might be interesting for metamorphic rocks containing marbles and calcium-silicate lithotypes [3]. The Mg/Ca ratio is used as a geothermometer to estimate the temperature of progressive metamorphism from calcite-dolomite solvus curve introduced by Harker & Tuttle [4] and Graf & Goldsmith [5]. Calcite + dolomite as geothermometers was characterized both experimentally and empirically by Goldsmith & Newton [6], Bickle & Powell [7], Powell [8], and Anovitz & Essene [9].

Research on the determination of seawater composition over geological time depends on the correct quantification of the Mg/Ca ratio in calcite. The percentage of Mg incorporated by marine

organisms is associated with temperature, so that when Mg content decreases in calcite, the seawater temperature might be interpreted as lower. In this case, the prior and accurate knowledge of the Mg/Ca ratio in the minerals that form the shells of marine organisms can determine a better correlation in the construction and interpretation of the sea water composition curve [10,11] and its effects on precipitated carbonate mineralogy [12].

Carbonates are dominant in the extensive pre-evaporitic oil and gas reservoirs related to the Atlantic rift opening in Brazil. The interplay of continental clastic and volcanogenic contributions [13–15], and carbonate precipitation strongly mediated by microorganisms [16], resulted in a large variety of rocks and its reequilibration of products based on carbonate minerals [17,18]. Its interpretation still represents a major challenge for oil companies requiring new exploratory models. The characterization and knowledge of calcite and dolomite crystallochemistry is also paramount for the interpretations of the reservoirs. Jones and Luth [19] observed a relationship between the porosity in dolomites and the composition of dolomite phases associated to excess Ca in its crystal structure, causing great rock heterogeneity.

Determination of the composition of calcite and dolomite in various rocks faces several unexpected limitations, due to its great compositional variability and the occurrence together with other minerals that bear Ca and Mg. Stoichiometric calculations based on whole-rock chemical analyses are thus not possible, and an elevated number of point analyses would be required to assess the whole range of compositions with statistical significance. Powder X-ray diffraction analysis, however, provides a convenient whole-rock analysis, able to determine and quantify all of the minerals in the sample, and has been used to track the variability of the carbonates' compositions. Determination of the Mg content in calcite was initially based on a single peak displacement in the diffraction pattern, as proposed by Chave [20] and Goldsmith et al. [21]. Goldsmith and Graf [22], Goldsmith et al. [23], and Erenburg [24] used other lattice parameters (cell volume and c/a ratio) for calibration. But, Milliman et al. [25] had already observed that this method could not be applied universally, and Althoff [1] questioned the accuracy of an analysis based on a single reflection of the diffraction pattern, while Bischoff et al. [26] proved an error of up to 5 mol % $MgCO_3$ for the method.

Bischoff et al. [26] and Mackenzie et al. [27] were the first to provide calibration based on the lattice parameters calculated by least squares regression, while Effenberger et al. [28], Markgraf & Reeder [29], Falini et al. [30], Reeder [31], and Titschack et al. [32], refined carbonate lattice parameters. Titschack et al. [32] proposed a new calibration to determine the Mg content in calcite by XRD and the Rietveld method, for samples with one or two generations of calcite composition. Nevertheless, previous studies had not addressed the determination of calcite (and dolomite) composition while quantifying all the minerals, requiring the previous purification of the sample.

This study aims at implementing a new method for quantification of the substitution of Mg for Ca at the A site of magnesian calcite and the excess of Ca located at the B site of non-stoichiometric dolomite, while performing a quantitative phase analysis. The X-ray diffraction and the fundamental parameters approach for the Rietveld refinement method on which this study is based, is fast and accurate, and provides the compositions of calcite and dolomite (more than one generation for each, if required) and the quantification of all minerals in the sample in one single operation.

2. Materials and Methods

Twenty-two samples from Brazilian sedimentary basins, such as a pisolitic limestone from Itaboraí (RJ), dolomite rock from Sergipe-Alagoas, carbonate stromatolites from Parnaíba (PI, MA, CE), stromatolite intercalated with calcarenite of Irecê (BA), and calcretes of Bauru (MG) were used. Recently grown microbial mats, precursor to carbonate stromatolites, were sampled from Lagoa Salgada and Lagoa Vermelha (RJ), and calcareous limestone and marble of the Candido Mountain Range (RJ), bioclastic granules from the Itapemirim coast (ES), and bioconstructions cemented by calcite on rocky shores of Arraial do Cabo (RJ). These samples were considered as analogous to the rocks of the

pre-evaporite petroleum system of Southeastern Brazil [33], and contain the calcite and dolomite with wide compositional ranges, allowing for the validation of the method.

X-ray diffraction patterns were generated in a D8 Advance Eco equipment (Bruker-AXS, Karlsruhe, Germany) under the following operating conditions: Cu Kα sealed tube (λ = 0.154056 nm) operated at 40 kV and 25 mA, measured from 4 to 105° 2θ at 0.01° step with a LynxEye XE energy-discriminant position sensitive detector. The identification of all minerals was performed with Bruker-AXS's Diffrac.EVA 4.0 or 4.1 software and PDF04+ database [34]. Full Rietveld method refinement, using fundamental parameters [35], was accomplished with DIFFRAC.TOPAS v.4.2 or 5.0 (Bruker-AXS, Karlsruhe, Germany) software. The background was modelled by 6th order polynomial, and the five Cu Kα emission lines of Berger [36] with an additional Kβ line from Hölzer et al. [37], were fitted, the contribution of the latter one refined to account for minor Kβ not eliminated by the detector. Other fitted instrumental parameters were a sample displacement and absorption.

Spot-sized chemical analyses were carried out on a Quanta 400 scanning electron microscope (FEI, Brno, Czech Republic), operated under high vacuum, 20 kV and spot size 5, coupled to a Bruker Nano Quantax 800 energy-dispersive X-ray fluorescence spectrometer (EDS) with XFlash 4030, 5010 or 6|60 detectors. Carbon from EDS analysis was calculated by stoichiometry both for calcite and dolomite. Point chemical analyses were also performed with a JXA-8230 Superprobe electron microprobe (EMPA) (JEOL, Tokyo, Japan) in WDS mode, at 15 kV, and 5 nA with a 10 µm beam using standards: CaF_2 for F, dolomite for Mg, Sr_AN for Sr, calcite for Ca, celsian for Ba, and siderite for Mn and Fe. Analyzer crystals and energy windows are in Table S1.

The total chemical composition of the sample was determined by X-ray fluorescence on an AXIOS spectrometer (Panalytical, Almelo, The Netherlands). Loss on ignition determination for each sample was supplied by thermogravimetry, accounting for the total mass loss from ~150 to 1200 °C, as described below. A LECO SC-632 elemental analyzer assayed the elemental carbon.

Thermogravimetric analysis was performed on a STAR^e System (Mettler-Toledo, Toledo, OH, USA) equipped with a GC 200 gas controller, under CO_2 atmosphere (analytical grade 4.8) with controlled flow rate of 50 mL/min, and a heating rate of 10 °C/min over the temperature range of 40 to 1200 °C.

3. Results

The experimental data of Goldsmith et al. [23] and Zhang et al. [38] related the Mg for Ca substitution in magnesian calcite to the lattice parameters *a* and *c*. Both relations are linear up to 0.287 Mg apfu, but the linearity does not extend to higher substitutions (Figure 1). The *c* axis correlates better, through the Equation:

$$c = -1.8603\ n\mathrm{Mg} + 17.061 \quad (1)$$

where *c* is the length of the crystallographic axis *c* (in Å), and *n*Mg is the molar fraction or number of atoms per formula unit(apfu) of Mg that replace Ca in calcite. Restraining the application of this equation for the *n*Mg range from 0.000 to 0.287 corresponds to *c* ranging from 17.061 to 16.528 Å, respectively (Table 1).

Table 1. Crystallographic cell parameters of Goldsmith et al. [23] and Zhang et al. [38] for calcite with variable Mg contents used to constrain the refinement of magnesian calcite.

$MgCO_3$ Molar Fraction	*a* (Å)	*c* (Å)
0.000	4.9900	17.061
0.100	4.9494	16.876
0.163	4.9297	16.754
0.287	4.8950	16.528

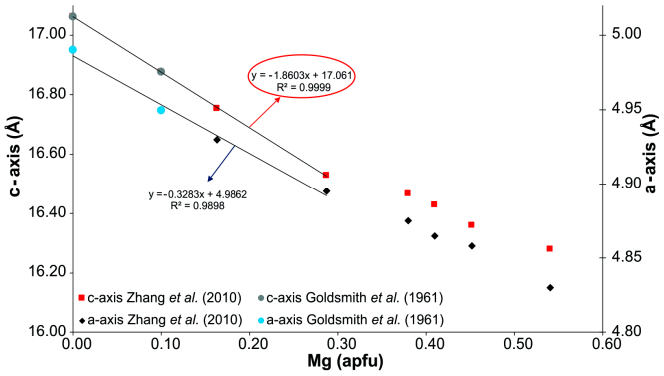

Figure 1. Dimensions of the crystallographic axes *a* and *c* and molar fraction of $MgCO_3$, and the respective equations of the lines with their R^2 figure of merit.

McCarthy et al. [39] present a similar approach for non-stoichiometric dolomite. The relationship between both of the crystallographic axes *a* and *c* of dolomite and the molar fraction of excess Ca, allocated on the B site of the mineral, is presented in Figure 2. Only Mg occupies the B site when the dolomite is stoichiometric. As for calcite, the *c* axis achieves a better correlation (factor of 0.9983), and relates to the excess Ca in the B site Δn_{Ca} by Equation (2):

$$c = c_o + 0.8632\Delta n_{Ca} \quad (2)$$

where *c* is the length of the crystallographic axis *c* and c_o is the length of the crystallographic axis when the dolomite is stoichiometric ($\Delta n_{Ca} = 0.00$). The lattice parameters *a* and *c* of McCarty et al. [39] ($a = 4.8071$ Å, $c = 16.0032$ Å), coincident with those calculated by Reeder and Sheppard [40], allow for Equation (2) to be rewritten as:

$$c = 16.0032 + 0.8632\Delta n_{Ca} \quad (3)$$

McCarthy et al. [39] discovered that, when excess Ca (Δn_{Ca}) in the dolomite exceed 0.07 (apfu), a second dolomite phase could be detected, and two well-delimited groups of dolomite might be observed (Figure 2). The authors defined the first, low excess-Ca dolomite, to occur in the range of the number of total Ca atoms from 1.00 to 1.10, high excess-Ca dolomite from 1.10 to 1.15 apfu, although their data supports the latter up to 1.25 apfu. With these well-established relationships, two different structures of non-stoichiometric dolomite were created, with the limit lattice parameters for the two phases as in Table 2.

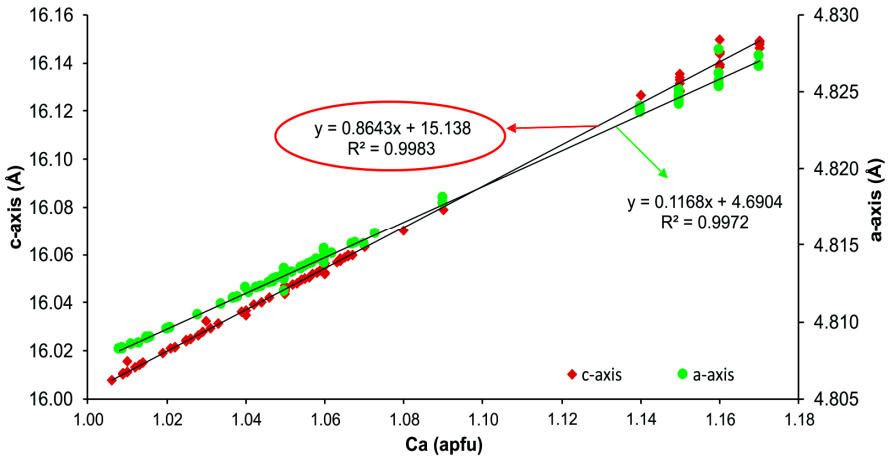

Figure 2. Relationship between the crystallographic axis *a* and *c* of Ca amount (*n*Ca), evidencing two groups of dolomite, modified from [39].

Table 2. Lattice parameters for dolomite generations implemented in the refinement software.

Phases	Parameters	Minimum	Maximum
Dolomite I (LCD)—low Ca-excess	a (Å)	4.8070	4.8187
	c (Å)	16.0032	16.0895
	Δn_{Ca}	0.00	0.10
Dolomite II (HCD)—high Ca-excess	a (Å)	4.8187	4.8362
	c (Å)	16.0895	16.2190
	Δn_{Ca}	0.10	0.25

The Equations (1) and (3) were implemented in the TOPAS software as a restriction to the XRD refinement of the cationic site occupancy by the Rietveld method, respectively, for the Mg-for-Ca isomorphic substitution in magnesian calcite and excess Ca in non-stoichiometric dolomite.

The results of the Rietveld method for all of the samples with the mineral quantification (% by mass), $MgCO_3$ molar fraction in magnesian calcite, molar fraction of excess $CaCO_3$ in non-stoichiometric dolomite (dolomite I and dolomite II), as well as the lattice parameters a and c, the position of the reflection d(104), and the cell volume, are presented in Table 3. The quality of the refinement is exemplified in Figure 3, choosing samples with large amounts of magnesian calcite and non-stoichiometric dolomite.

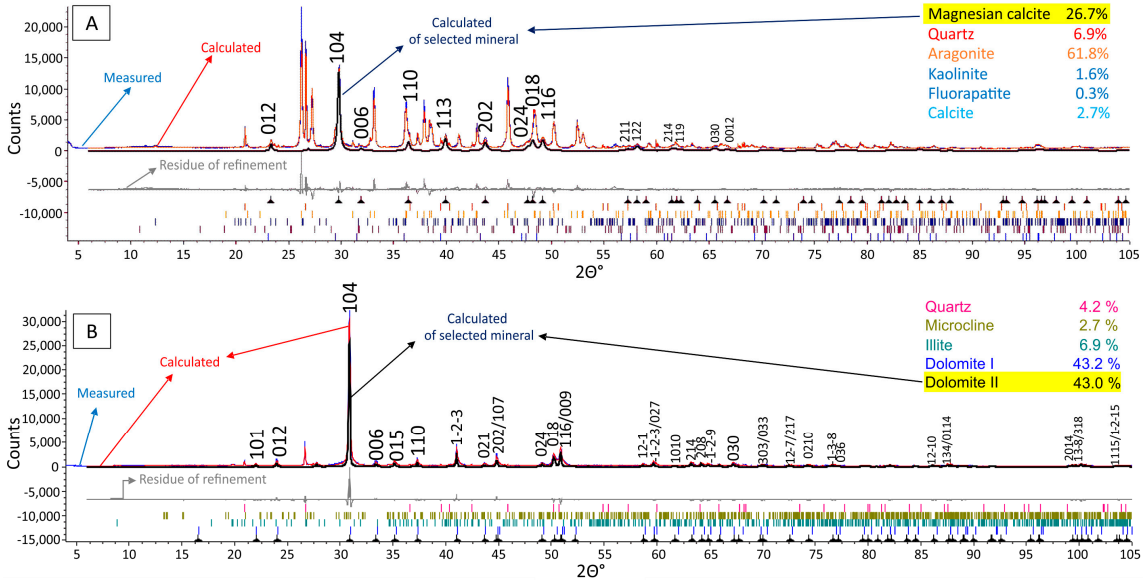

Figure 3. Refinement result for samples with the abundant (**A**) magnesian calcite in sample AC3623 and (**B**) non-stoichiometric dolomite in sample C14. The blue and red curves are measured and calculated diffraction pattern, respectively. The black curve is the diffraction pattern for the highlighted mineral. The gray curve is the residue of the refinement, followed by the position of the crystallographic reflections of quantified minerals following order and color code of the list in the upper right corner. The miller indexes for reflections refer to the highlighted minerals in (**A**,**B**).

Table 3. Mineral quantification based on XRD and fundamental parameter Rietveld refinement (wt %), as well as the molar fraction of Mg-for-Ca substitution in calcite and the $CaCO_3$ excess in non-stoichiometric low calcium-excess (dolomite I) and high calcium-excess (dolomite II) dolomite.

	Mineral	EC01	PS01	04	05	07	10	Lithot	LV07	LS	C12	C14	PA2B	PA5C	PA13	PA17	AC 0370	AC 0371	AC 0372	AC 3623	Am1c	Am2a	2B
	Dolomite		12.3				3.3								0.9								
	Dolomite I		55.9				23.4				21.7	43.2		5.2	19.6	7.8							
	Dolomite II						10.7		2.3			43.0		7.8	10.4	6.5						3.1	
	Calcite	5.9	6.0	11.3	43.4	28.4		3.8		3.1	22.6		28.0	5.2	6.3	19.8	4.1		4.8	2.7	3.4	4.8	36.8
	Calcite-Mg	93.5	23.1	85.0	55.0	68.5	46.0	61.6	78.5	13.6	42.0		47.2	62.9	4.4	42.5	76.9	86.3	72.4	26.7	31.4	35.9	23.6
	Aragonite							32.7	17.8	76.4							13.8	8.7	14.8	61.8	62.1	54.1	36.5
	Quartz	0.6	0.7	3.7	1.5	0.3	5.9	0.7	1.5	5.0	8.2	4.2	12.7	10.4	58.4	12.0	5.3	5.0	7.9	6.9	1.8	0.9	3.0
	Gypsum																				1.2	0.4	
	Fluorapatite						1.3	0.6												0.3			
	Microcline		0.2				8.6	0.7		1.9	4.1	2.7	3.6	4.1		4.2							
	Pyrite					0.4	0.6																
	Chlorite													0.7									
	Actinolite		1.3																				
	Muscovite		0.4				0.4				0.5												
	Illite					2.0					0.6	6.9	3.1	3.8		6.2							
	Montmorillonite					0.4																	
	Kaolinite										0.3									1.6		0.9	
	Palygorskite												1.4			1.1							
	Glauconite												4.0										
	Talc		0.2																				
	Total	100.0	100.0	100.0	100.0	100.0	100.0	100.0	100.0	100.0	100.0	100.0	100.0	100.0	100.0	100.0	100.0	100.0	100.0	100.0	100.0	100.0	100.0
	Lattice parameters																						
Calcite-Mg	a (Å)	4.981	4.966	4.984	4.986	4.983	4.985	4.933	4.919	4.940	4.983		4.984	4.982	4.981	4.981	4.929	4.934	4.932	4.932	4.930	4.931	4.957
	c (Å)	17.021	16.960	17.041	17.047	17.027	17.045	16.808	16.747	16.859	17.035		17.036	17.027	16.995	17.023	16.786	16.806	16.800	16.813	16.792	16.801	16.929
	d104 (Å)	3.03	3.02	3.03	3.03	3.03	3.03	3.00	2.99	3.00	3.03		3.03	3.03	3.03	3.03	2.99	3.00	2.99	3.00	2.99	2.99	3.01
	cell volume	365.7	362.3	366.6	367.0	366.1	366.7	354.2	351.0	356.3	366.3		366.5	367.0	365.2	365.8	353.2	354.3	354.0	354.2	353.4	353.8	360.3
	Molar fraction $MgCO_3$	0.02	0.05	0.01	0.01	0.02	0.01	0.14	0.17	0.11	0.01		0.01	0.02	0.04	0.02	0.15	0.14	0.14	0.13	0.14	0.14	0.07
Dolomite I	a (Å)		4.813				4.809					4.812		4.819	4.815	4.819							
	c (Å)		16.039				16.009					16.033		16.086	16.062	16.071							
	d104 (Å)		2.89				2.89					2.89		2.90	2.89	2.89							
	cell volume		321.8				320.7					321.5		323.5	322.5	322.2							
	Molar fraction $CaCO_3$ (excess)		0.04				0.01					0.03		0.10	0.07	0.08							
Dolomite II	a (Å)						4.819		4.836		4.827	4.820		4.834	4.831	4.827							
	c (Å)						16.090		16.219		16.139	16.109		16.169	16.156	16.145						16.219	
	d104 (Å)						2.90		2.91		2.90	2.90		2.91	2.91	2.90						2.91	
	cell volume						323.5		328.5		325.6	324.1		327.2	326.5	325.8						328.5	
	Molar fraction $CaCO_3$ (excess)						0.10		0.25		0.16	0.12		0.19	0.18	0.16						0.25	

The conciliation of the chemical composition calculated from the XRD results against X-ray fluorescence analyses (XRF) is graphically shown in Figure 4A, while Figure 4B emphasizes Ca and Mg, the elements calculated directly from the structure of the carbonates. It is assumed that some deviation in the conciliation is due to several other minerals besides the carbonates, while the calculated Mg values, whose bearers are exclusively the fitted carbonates, match the chemical analyses very well.

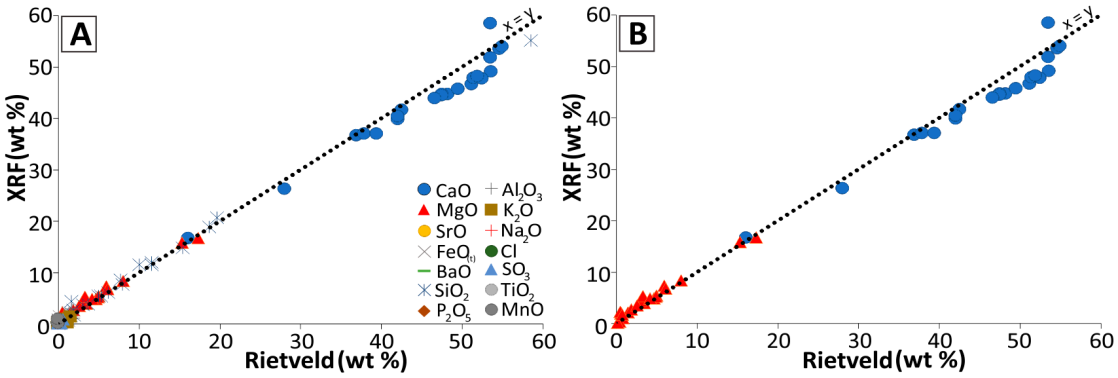

Figure 4. Conciliation of the chemical composition derived from mineral quantification by the Rietveld method (XRD) against XRF analyses (wt %). (**A**) Data for all analyzed elements. (**B**) Data only for Ca and Mg. Data in Tables S2 and S3.

The results of the Rietveld method refinement were further checked against C measured by the elemental analysis and CO_2 determined by thermogravimetry under CO_2 atmosphere, which separates the thermal events of mass loss of the carbonate from the magnesite molecule due to dolomite from calcite [41], in Figure 5.

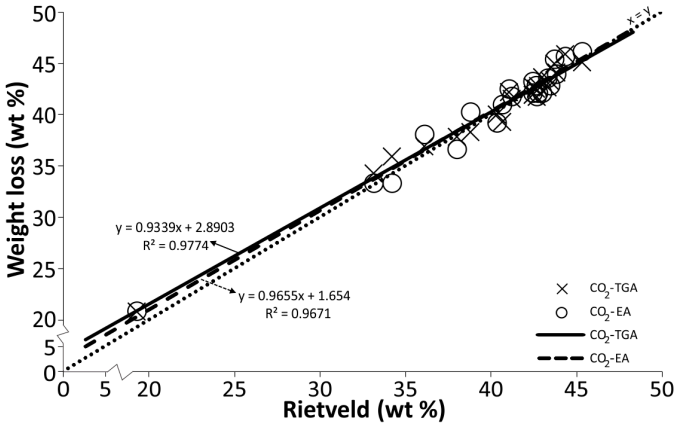

Figure 5. Conciliation of the CO_2 content derived from mineral quantification by the Rietveld method (XRD) against CO_2 mass loss by thermogravimetry (TGA) represented by X and with elemental carbon (presented as CO_2) as measured by elemental analysis (EA) represented by circles (wt %). Data in Table S4.

Other analytical techniques were also used to compare the results and validate the proposed method. Analyzes by EDS and WDS demonstrate that the carbonates' compositional range for each sample might be very large. Figure 6 shows EDS results for 2617 point chemical analyses, grouping a few samples for clearer visualization, as compared to the results of refinement by the Rietveld method. The blue dashed lines show the compositional upper limit of the method for magnesian calcite (MC) at 0.287 Mg apfu, and the lower limits for dolomite I (low calcium-excess dolomite—LCD, 0.900 Mg apfu), and dolomite II (high calcium-excess dolomite, HCD—0.750 Mg apfu).

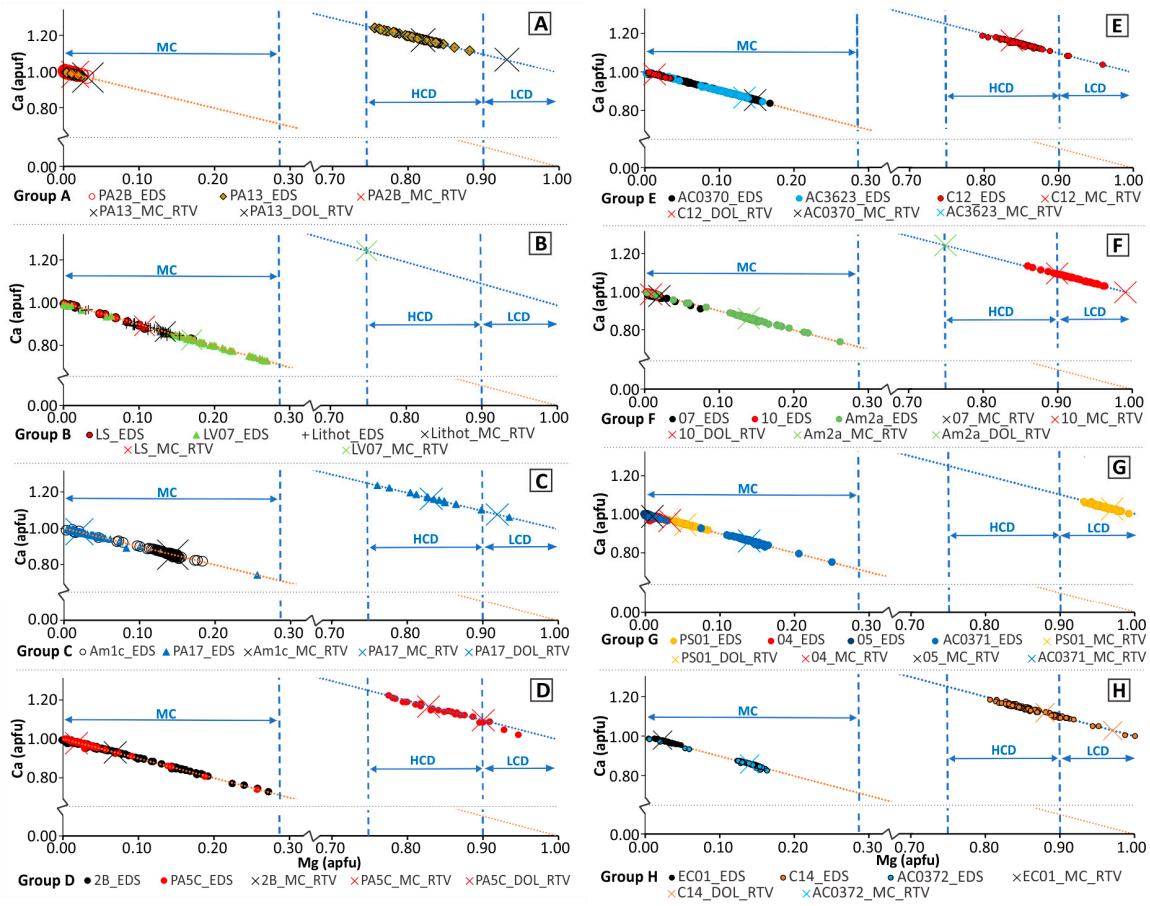

Figure 6. Results of energy-dispersive X-ray fluorescence spectrometer (EDS) analyses represented by circles, triangles, and diamonds, as compared to the Rietveld method (RTV) results represented by X, for magnesian calcite (MC), low calcium dolomite I (LCD), and high calcium dolomite II (HCD). (**A**–**H**) Different groups of samples separated for clearer visualization. Data in Table S5.

The general agreement of the refined results with the point analysis is excellent. XRD is a bulk method, and therefore is able to accommodate for the compositional variations while refining. It will retrieve the mean composition for the carbonates for every compositional domain. Point analysis, on the other hand, is spatially limited to a few micrometers of the volume excited by the electron beam, and a larger number of analyses are required to encompass the whole range. Almost all compositions refined from the XRD plot in the range, as determined by EDS. A few exceptions occur, however. Examples are given in Figure 6B,F, where non-stoichiometric dolomite II, with 0.25 apfu excess of Ca, was refined by the Rietveld method for samples, respectively, LV07 and Am2a, but was not detected by EDS; this is due to the low grade of the mineral in the sample, only 2.3% and 3.1%, respectively (Table 3), but within the detection limit of XRD. The same happens to sample PA13 (Figure 6A), where dolomite I could not be detected by EDS. Careful reanalysis of the sample (Figure 7) showed the fine intergrowth with dominant (58.4%) quartz (Table 3). Intergrowth and fine particle size is not limiting XRD-based analysis.

Some samples (EC01, PS01, 04, 10, Lithot, C12, C14, AC0370, AC3623, Am2a, PA13, and PA2B) were selected for point chemical analysis by electron microprobe analysis (EMPA). Figure 8 shows the composition of the samples, again comparing it with the refinement result by the Rietveld method. As for the EDS analysis, no dolomite II could be found in sample Am2a (Figure 8C), due to the low content of the phase. The significantly smaller number of analyzed points (163), to some extent, reduces

the range of sampled compositions, but mostly the Rietveld refinement results also plot among the chemical analyses for each sample.

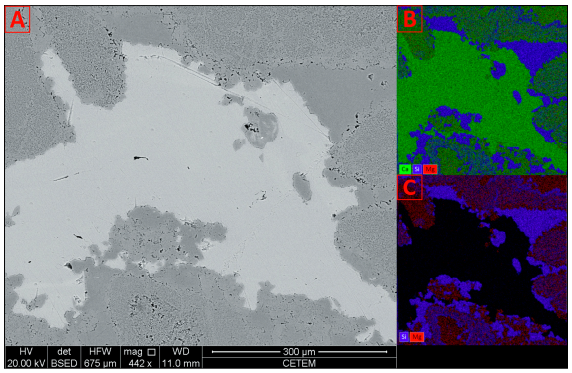

Figure 7. Sample PA13, (**A**) backscattered electrons image with brighter calcite, "smooth" gray quartz and dolomite; (**B**) dot map for Ca, Si and Mg, showing blue quartz, light green calcite and dominant dolomite II in dark green. A small, darker, area at the bottom shows a higher Mg content, corresponding to dolomite I; (**C**) dot map only for Si and Mg, showing blue quartz and red dolomite II. The dolomite I area at the bottom also contains higher Si contents, and is interpreted as sub-micrometric intergrowth of dolomite with quartz.

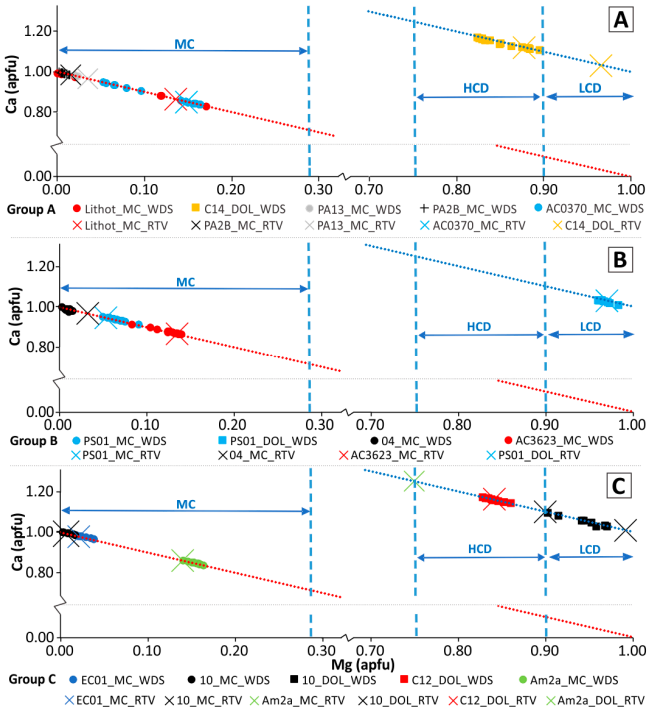

Figure 8. Results of EMPA (WDS) analyses represented by circles, triangles and diamonds, compared to the Rietveld (RTV) method represented by X for magnesian calcite (MC), dolomite I (LCD) and dolomite II (HCD). (**A**–**C**) Different groups of samples separated for clearer visualization. Data in Table S6.

It should be stressed that the perfect alignment of the analyses on the theoretical lines in Figures 6 and 8 is due to the calculation $\left(X_{Ca}^{cal} + X_{Mg}^{cal} = 1\right)$ for calcite, where the total atoms for the A site is equal to 1, and $\left(X_{Ca}^{dol} + X_{Mg}^{dol} = 2\right)$ for 2 atoms at sites A + B in dolomite.

4. Discussion

Titschack et al. [32] also used a fundamental parameters approach to the Rietveld method for magnesian calcite quantification, starting refinement with the structure defined by Paquette & Reeder [42], with molar fraction of 0.129 $MgCO_3$. After retrieving the refined lattice parameters and plotting them against the chemical analyses of his samples, they used a calibration curve based on cell volume to calculate the Mg and Ca site occupancy, adjusting these values in the software for phase quantification. The results obtained by Titschack et al. [32] are compared to those of the present work in Figure 9. Both of these studies display very close results, with similar correlation coefficients. Rather than dynamically constraining the Mg-for-Ca substitution, Titschack et al. [32] applied a two-step refining routine, i.e., refining lattice parameters, using them to determine substitution, and then adjusting the occupancy in the structure for further operations. The authors also discuss the possibility of multiple calcite compositions in the samples, and use their method to quantify the (simulated) binary mixtures. It was a very fortuitous case study, as the echinoid remains (coronas and spines) contained exclusively magnesian calcite of uniform composition, allowing them to use the whole-sample ICP-AES chemical analysis after full dissolution to correlate them to the lattice parameters. These are high-quality data on magnesian calcite.

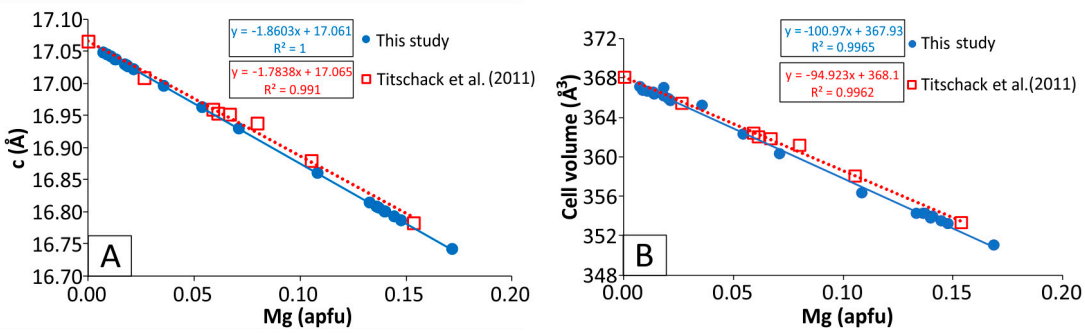

Figure 9. Comparing correlation of lattice parameters for magnesian calcite of this study (in blue) and of Titschack et al. [32] (in red). (**A**) Correlation between crystallographic axis *c* and molar fraction of $MgCO_3$; (**B**) Correlations between cell volume and molar fraction of $MgCO_3$.

Comparison of the results of our study with different calibrations [22–24,26,27,30,32,42] for determination of the molar fraction of $MgCO_3$ in calcite shows that the new calibration is in agreement with the trend of the former publications (Figure 10), except for the c/a relation, as already observed by Titschack et al. [32]. Some authors validate this linear relationship only up to 0.18 apfu of Mg [20,27], stating that the relation is not linear any more above this content. Our data, based mostly on data of Goldsmith et al. [23] and Zhang et al. [38], extends the linear relation continuously up to 0.287 apfu of Mg.

The method for quantifying the substitution of Mg for Ca at the A site of magnesian calcite (up to 0.287 apfu) and the excess of Ca, located at the B site in non-stoichiometric dolomite (up to 0.25 apfu) was applied and validated in different rocks samples from diverse geological environments with varied mineralogy.

In addition to having obtained a high degree of data correlation, the implemented method is fast, efficient, and refines more than one generation for calcite and dolomite, considering all of the reflections of each mineral phase. The new method convolutes the entire X-ray diffraction pattern, making quantification possible when the mineralogy is complex, even with peaks overlapping.

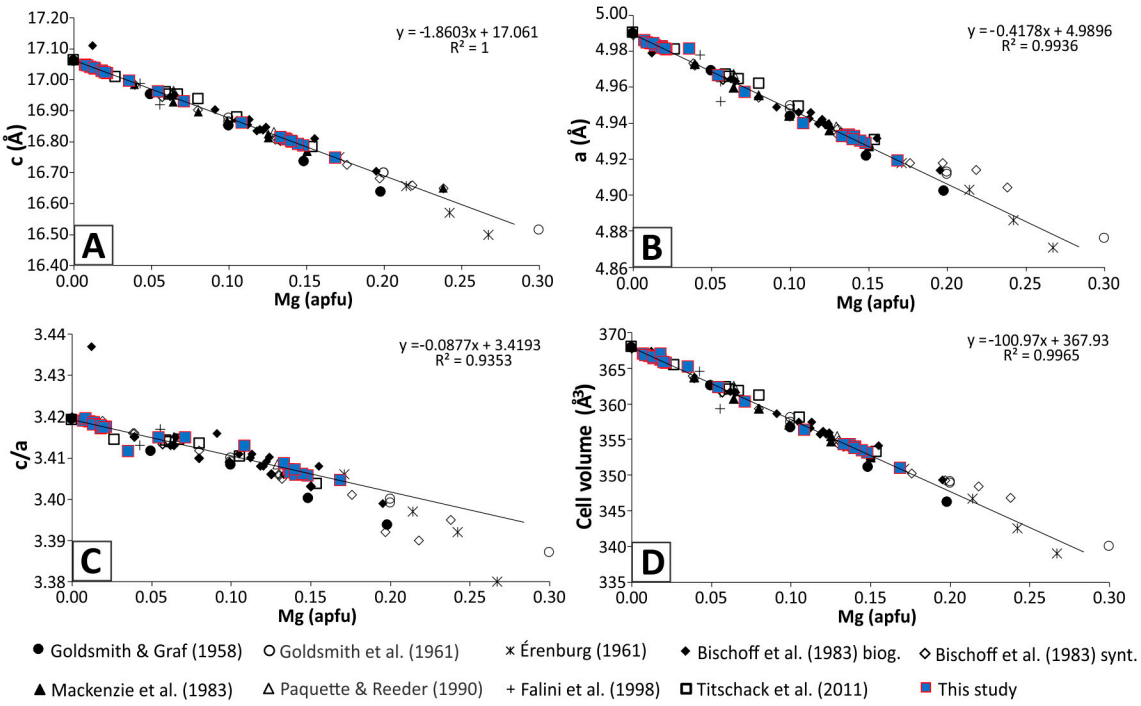

Figure 10. Plot of Mg content in magnesian calcite against lattice parameters from published data. Data of our study are represented as blue squares with red border. The equation of the line and correlation coefficient R^2 refers to the data of our study. (**A**) Correlation of the length of crystallographic axis *c* and molar fraction of $MgCO_3$; (**B**) Correlation of the length of crystallographic axis *a* and molar fraction of $MgCO_3$; (**C**) Correlation of ratio *c*/*a* of the crystallographic axes and molar fraction of $MgCO_3$; and, (**D**) Correlation of cell volume and molar fraction of $MgCO_3$.

As always when using the Rietveld method, a comprehensive knowledge of the mineralogy of the sample prior to quantification is a requirement. Another paramount necessity is using the structure files that really describe the refined minerals. For mixed crystals, as in samples studied here, choosing adequate structures was not an easy task, and was used to require a multistep approach as the one adopted by Titschack et al. [32] for magnesian calcite. If solid solutions are a part of samples with complex mineralogy, the initial cell parameters refinement without constraints on occupancy can easily retrieve approximate values, leading to wrong occupancy. Refining occupation while constraining it to a lattice parameter allows a one-step procedure for the fundamental parameters of the Rietveld method refinement. Refining the occupancy provides a much better structure for the method to find real minima, and this gives improved results for the overall mineral quantification, as the effect of different scattering powers of Mg and Ca on intensities, i.e., scale factors, is taken into consideration. Titschack et al. [32] had already drawn attention to the possible bias of not considering the effect of scattering powers, which can be circumvented by our method. Exactly the same approach discussed for calcite has also been adopted for dolomite in this study.

By applying self-contained structures, which refine to its correct parameters, it is also possible to use it for more than one compositional variety in a sample, by setting precise lattice parameter limits. Here, we defined only one magnesian calcite variety with $MgCO_3$ allowed to refine between >0.000 to 0.287 apfu following the compositional range as defined by Goldsmith et al. [23] and Zhang et al. [38], but it is usually refined together with stoichiometric calcite. For dolomite, we have defined two varieties, low calcium-excess (LCD, >0.00 to 0.10) and high calcium-excess (HCD, >0.10 to 0.25) dolomite, as adopted by McCarthy et al. [39], usually refined together with stoichiometric dolomite. The limits of the varieties could be shifted, as the equations are valid throughout the entire compositional range, and the inclusion of another variety could be considered, if the limits are well defined.

While potentially providing more information than competing techniques, X-ray diffraction with the Rietveld method analysis is still cost-effective and competitive. As discussed before, spot chemical analysis by EMPA or EDS might require a large number of analyzed points for statistical reasons, which increase both time and costs. Bulk sample chemical analysis is cheaper, but the reach of the results is impaired by complex mineralogy. Nevertheless, it is recommended to combine chemical and XRD analysis, as the conciliation of results greatly adds to its reliability.

5. Conclusions

We implemented a method for quantifying the substitution of Mg for Ca in magnesian calcite and the excess of Ca in non-stoichiometric dolomite by the constrained Rietveld method refinement of X-ray diffraction spectra, while performing quantitative phase analysis.

The tool developed in this work allows for the generation of high quality quantitative mineralogical data, with unprecedented detail on the composition of Ca and Mg carbonates. Despite the restrictions imposed onto carbonate composition, $X_{Mg} \leq 0.287$ for high-Mg calcite and $X_{Mg} \geq 0.75$ for high-Ca dolomite, most samples could be refined within these limits. The original data we used to define the tool, however, precludes its application to extreme substitutions.

Samples derived from the petroleum systems show the most significant Mg substitutions for Ca in calcite and Ca excess replacing Mg at the B site of dolomite. Validation analyses of the method with samples of petroleum systems constitute an excellent case study. As pointed out by Wright [17], a large range of carbonates with Mg in the crystal structure might be produced in lakes with volcanic influence, especially in rift settings as those of the pre-salt rocks in Southeastern Brazil. The capability of determining the complete mineralogy by a fast and reliable method allows for the generation of the great amount of data needed to adequately interpret the deposition environment and further evolution, thus fostering better prospective models for exploration.

Supplementary Materials: The following are available online at www.mdpi.com/2075-163X/7/9/164/s1, Table S1: Analytical parameters for EMPA (WDS), Table S2: Data as plotted in Figure 4: chemical composition as calculated from mineral quantification by the Rietveld method (wt %), Table S3: Data as plotted in Figure 4: results from XRF analysis in wt %, Table S4: Data as plotted in Figure 5: CO_2 content from different methods, Table S5: Data as plotted in Figure 6: EDS analysis of calcite and dolomite and structural formula, Table S6: Data as plotted in Figure 8: WDS analysis of calcite and dolomite and structural formula.

Acknowledgments: This paper is dedicated to the memory of Hugo M. Rietveld (1932–2016), whose method still inspires new applications, after 50 years. The authors thank Lagesed/UFRJ, Nacional Museum/UFRJ and Carolina Keim for the petroleum system samples, Ivan Araújo and José Brod for EPMA analyses at the Regional Center for Development, Technology and Innovation (CRTI), and PPGL/UFRJ. CNPq is thanked for scholarship (Hélisson Santos) and financial support to Ciro Ávila and Reiner Neumann, as well as to the project 483387/2013-4. Comments and suggestion from two anonymous reviewers substantially improved our text.

Author Contributions: Hélisson Santos performed the experiments, located adequate samples and wrote the paper; Reiner Neumann conceived the experiments; Ciro Ávila checked data consistency and presentation, and contributed to the final text. All authors analyzed the data and worked to improve the paper.

Conflicts of Interest: The authors declare no conflict of interest.

References

1. Althoff, P.L. Structural refinements of dolomite and a magnesian calcite and implications for dolomite formation in the marine environment. *Am. Mineral.* **1977**, *62*, 772–783.
2. Helpa, V.; Rybacki, E.; Morales, L.F.G.; Dresen, G. Influence of grain size, water, and deformation on dolomite reaction rim formation. *Am. Mineral.* **2016**, *101*, 2655–2665. [CrossRef]
3. Letargo, C.M.; Lamb, W.M.; Park, J.S. Comparison of calcite + dolomite thermometry and carbonate + silicate equilibria: Constraints on the conditions of metamorphism of the Llano uplift, central Texas, USA. *Am. Mineral.* **1995**, *80*, 131–143. [CrossRef]
4. Harker, R.I.; Tuttle, O.F. Studies in the system CaO-MgO-CO_2; Part 2, Limits of solid solution along the binary join $CaCO_3$-$MgCO_3$. *Am. J. Sci.* **1955**, *253*, 274–282. [CrossRef]

5. Graf, D.L.; Goldsmith, J.R. Dolomite-magnesian calcite relations at elevated temperatures and CO_2 pressures. *Geochim. Cosmochim. Acta* **1955**, *7*, 109. [CrossRef]
6. Goldsmith, J.R.; Newton, R.C. P-T-X relations in the system $CaCO_3$,-$MgCO_3$, at high temperatures and pressures. *Am. J. Sci.* **1969**, *267*, 160–190.
7. Bickle, M.J.; Powell, R. Calcite-dolomite geothermometry for iron-bearing carbonates. *Contrib. Mineral. Petrol.* **1977**, *59*, 281–292. [CrossRef]
8. Powell, R.; Condliffe, D.M.; Condliffe, E. Calcite–dolomite geothermometry in the system $CaCO_3$–$MgCO_3$–$FeCO_3$: An experimental study. *J. Metamorph. Geol.* **1984**, *2*, 33–41. [CrossRef]
9. Anovitz, L.M.; Essene, E.J. Phase equilibria in the system $CaCO_3$-$MgCO_3$-$FeCO_3$. *J. Petrol.* **1987**, *28*, 389–415. [CrossRef]
10. Stanley, S.M.; Ries, J.B.; Hardie, L.A. Low-magnesium calcite produced by coralline algae in seawater of Late Cretaceous composition. *Proc. Natl. Acad. Sci. USA* **2002**, *99*, 15323–15326. [CrossRef] [PubMed]
11. Ries, J.B. Mg fractionation in crustose coralline algae: Geochemical, biological, and sedimentological implications of secular variation in the Mg/Ca ratio of seawater. *Geochim. Cosmochim. Acta* **2006**, *70*, 891–900. [CrossRef]
12. Hardie, L.A. Secular variation in seawater chemistry: An explanation for the coupled secular variation in the mineralogies of marine limestones and potash evaporites over the past 600 my. *Geology* **1996**, *24*, 279–283. [CrossRef]
13. Muniz, M.C.; Bosence, D.W.J. Pre-salt microbialites from the Campos Basin (offshore Brazil): Image log facies, facies model and cyclicity in lacustrine carbonates. *Geol. Soc. Spec. Publ.* **2015**, *418*, 221–242. [CrossRef]
14. Carminatti, M.; Wolff, B.; Gamboa, L. New exploratory frontiers in Brazil. In Proceedings of the 19th World Petroleum Congress, Madrid, Spain, 29 June–3 July 2008.
15. Gomes, P.O.; Kilsdonk, B.; Minken, J.; Grow, T.; Barragan, R. The outer high of the Santos Basin, Southern Sao Paulo Plateau, Brazil: Pre-salt exploration outbreak, paleogeographic setting, and evolution of the syn-rift structures. In Proceedings of the AAPG International Conference and Exhibition, Cape Town, South Africa, 26–29 October 2008.
16. Jones, B.; Renaut, R.W. Calcareous spring deposits in continental settings. *Dev. Sedimentol.* **2010**, *61*, 177–224. [CrossRef]
17. Wright, V.P. Lacustrine carbonates in rift settings: The interaction of volcanic and microbial processes on carbonate deposition. *Geol. Soc.* **2012**, *370*, 39–47. [CrossRef]
18. Veysey, J.; Fouke, B.W.; Kandianis, M.T.; Schickel, T.J.; Johnson, R.W.; Goldenfeld, N. Reconstruction of water temperature, pH, and flux of ancient hot springs from travertine depositional facies. *J. Sediment. Res.* **2008**, *78*, 69–76. [CrossRef]
19. Jones, B.; Luth, R.W. Petrography of finely crystalline Cenozoic dolostones as revealed by backscatter electron imaging: Case study of the Cayman Formation (Miocene), Grand Cayman, British West Indies. *J. Sediment. Res.* **2003**, *73*, 1022–1035. [CrossRef]
20. Chave, K.E. A solid solution between calcite and dolomite. *J. Geol.* **1952**, *60*, 190–192. [CrossRef]
21. Goldsmith, J.R.; Graf, D.L.; Joensuu, O. The occurrence of magnesian calcite in nature. *Geochim. Cosmochim. Acta* **1955**, *7*, 212–230. [CrossRef]
22. Goldsmith, J.R.; Graf, D.L. Relation between lattice constants and composition of the Ca-Mg carbonates. *Am. Mineral.* **1958**, *43*, 84–101.
23. Goldsmith, J.R.; Graf, D.L.; Heard, H.C. Lattice constants of the calcium-magnesium carbonates. *Am. Mineral.* **1961**, *46*, 453–459.
24. Érenburg, B.G. Artificial mixed carbonates in the $CaCO_3-MgCO_3$ series. *J. Struct. Chem.* **1961**, *2*, 167–171. [CrossRef]
25. Milliman, J.D.; Gastner, M.; Müller, J. Utilization of magnesium in coralline algae. *Geol. Soc. Am. Bull.* **1971**, *82*, 573–580. [CrossRef]
26. Bischoff, W.D.; Bishop, F.C.; Mackenzie, F.T. Biogenically produced magnesian calcite: Inhomogeneities in chemical and physical properties; comparison with synthetic phases. *Am. Mineral.* **1983**, *68*, 1183–1188.
27. Mackenzie, F.T.; Bischoff, W.D.; Bishop, F.C.; Loijens, M.; Choonmaker, J.; Wollast, R. Magnesium calcites: Low-temperature occurrence, solubility and solid-solution behavior. *Rev. Mineral. Geochem.* **1983**, *11*, 97–144.
28. Effenberger, H.; Mereiter, K.; Zemann, J. Crystal structure refinements of magnesite, calcite, rhodochrosite, siderite, smithonite, and dolomite, with discussion of some aspects of the stereochemistry of calcite type carbonates. *Z. Krist-Cryst. Mater.* **1981**, *156*, 233–244. [CrossRef]

29. Markgraf, S.A.; Reeder, R.J. High-temperature structure refinements of calcite and magnesite. *Am. Mineral.* **1985**, *70*, 590–600.
30. Falini, G.; Fermani, S.; Gazzano, M.; Ripamonti, A. Structure and morphology of synthetic magnesium calcite. *J. Mater. Chem.* **1998**, *8*, 1061–1065. [CrossRef]
31. Reeder, R.J. Constraints on cation order in calcium-rich sedimentary dolomite. *Aquat. Geochem.* **2000**, *6*, 213–226. [CrossRef]
32. Titschack, J.; Goetz-Neunhoeffer, F.; Neubauer, J. Magnesium quantification in calcites [(Ca, Mg)CO_3] by Rietveld-based XRD analysis: Revisiting a well-established method. *Am. Mineral.* **2011**, *96*, 1028–1038. [CrossRef]
33. Terra, G.J.S.; Spadini, A.R.; França, A.B.; Sombra, C.L.; Zambonato, E.E.; Juschaks, L.C.S.; Arienti, L.C.; Erthal, M.M.; Blauth, M.; Franco, M.P. Classificações clássicas de rochas carbonáticas. *Bol. Geoci. Petrobras* **2010**, *18*, 9–29.
34. International Centre for Diffraction Data (ICDD). International Centre for Diffraction Data—PDF4+ Relational Powder Diffraction File. Available online: http://www.icdd.com/products/pdf4.htm (accessed on 8 September 2017).
35. Cheary, R.W.; Coelho, A. A fundamental parameters approach to X-ray line-profile fitting. *J. Appl. Crystallogr.* **1992**, *25*, 109–121. [CrossRef]
36. Berger, H. Study of the Kα emission spectrum of copper. *X-ray Spectrom.* **1986**, *15*, 241–243. [CrossRef]
37. Hölzer, G.; Fritsch, M.; Deutsch, M.; Hartwig, J.; Forster, E. K alpha1,2 and K beta1,3 X-ray emission lines of the 3d transition metals. *Phys. Rev. A.* **1997**, *56*, 4554–4568. [CrossRef]
38. Zhang, F.; Xu, H.; Konishi, H.; Roden, E.E. A Relationship between d104 value and composition in the calcite-disordered dolomite solid-solution series. *Am. Mineral.* **2010**, *95*, 1650–1656. [CrossRef]
39. McCarty, D.K.; Drits, V.A.; Sakharov, B. Relationship between composition and lattice parameters of some sedimentary dolomite varieties. *Eur. J. Mineral.* **2006**, *18*, 611–627. [CrossRef]
40. Reeder, R.J.; Sheppard, C.E. Variation of lattice parameters in some sedimentary dolomites. *Am. Mineral.* **1984**, *69*, 520–527.
41. Földvári, M. Handbook of the thermogravimetric system of minerals and its use in geological practice. In *Occasional Papers of the Geological Institute of Hungary*; Gyula, M., Ed.; Geological Institute of Hungary: Budapest, Hungary, 2011; Volume 213, p. 180; ISBN 978-963-671-288-4.
42. Paquette, J.; Reeder, R.J. Single-cristal X-ray structure refinements of two biogenic magnesian calcite crytals. *Am. Mineral.* **1990**, *75*, 1151–1158.